Phyton-
International Journal of
Experimental Botany

Tech Science Press

http://doi.org/10.32604/phyton.2026.067796

ARTICLE

A Transcriptional Suppressor NTL8 Interacts with CONSTANS to Control Photoperiod-Mediated Flowering Time in *Arabidopsis thaliana*

Yue Jin[1], Xiaoying Tang[1], Bingke Wei[1], Lulu Zhi[1], Yan Mao[1], García-Caparrós Pedro[2,*] and Xiangyang Hu[1,*]

[1]Shanghai Key Laboratory of Bio-Energy Crops, School of Life Sciences, Shanghai University, Shanghai, China
[2]Department of Agronomy, University of Almeria, Almeria, Spain
*Corresponding Authors: García-Caparrós Pedro. Email: pedrogar123@hotmail.com;
Xiangyang Hu. Email: huxiangyang@shu.edu.cn

Received: 13 May 2025; Accepted: 28 January 2026; Published: 31 March 2026

ABSTRACT: Plants perceive rhythmic photoperiodic signals to modulate flowering time. In *Arabidopsis thaliana*, long-day light conditions accelerate flowering through CONSTANS (CO)-activated FLOWERING LOCUS T (FT) signal pathway. The CO protein abundance presents circadian oscillation, enabling precise regulation of *FT* transcription. NTL8 belongs to the NAC transcription factor family and is reported to control leaf trichome development. Here, we reported that NTL8 regulated flowering time in Arabidopsis, because overexpressing *NTL8* significantly delayed flowering time, whereas loss-of-function mutant of *NTL8* accelerated flowering time. *NTL8* also presented circadian expression, maintaining elevated transcript levels during the daytime. Biochemical and genetic analyses revealed that NTL8 physically interacted with CO *in planta*, thereby antagonizing CO activity and repressing *FT* expression to delay the flowering time. Furthermore, overexpressing *NTL8* reduced the protein stability of CO, particularly by attenuating CO accumulation in the morning time and promoting CO degradation during the night. Collectively, our findings indicated that NTL8 delayed photoperiod-dependent flowering time by suppressing CO-mediated activation of *FT* expression and destabilizing CO protein. This study uncovers a previously unrecognized role for NTL8 in coordinating circadian and photoperiodic signals to fine-tune flowering time in *Arabidopsis thaliana*.

KEYWORDS: Arabidopsis; NTL8; CONSTANS; flowering time

1 Introduction

Flowering at the appropriate time leads to successful fertilization and seed production, thereby ensuring optimal crop yield [1–5]. Plant flowering time is accurately controlled by a complicated etwork of endogenous physiological signals as well as external environmental cues [4,6]. Among these, plants sense the day length via the photoperiodic pathway, also called photoperiod-mediated flowering time, which is controlled by the activity of the B-box protein CONSTANS (CO) in leaf phloem companion cells [6,7]. Transcription of *CO* is governed by the circadian clock, resulting in a rhythmic oscillation of its transcript level [4,8]. The proper functioning of CO also relies on its degradation through the ubiquitin-proteasome system at nighttime and dawn, allowing maximal CO levels to be reached near sunset in long photoperiods (16-h illumination/8-h darkness) [8–11]. The accumulated CO subsequently triggers the transcription of the flowering hormone gene FLOWERING LOCUS T (FT) within the vascular tissues of leaves [12–14]. The florigenic FT peptide subsequently functions

as a mobile developmental cue, moving to the shoot apex where it induces downstream flowering genes including APETALA1 (AP1) and LEAFY (LFY), ultimately triggering floral bud development in the reproductive apex [5,14,15]. Multiple transcriptional regulators influence CO abundance and activity. FLOWERING bHLH (FBH) and TEOSINTE BRANCHED 1/CYCLOIDEA/PROLIFERATING CELL NUCLEAR ANTIGEN FACTOR (TCP) TCP4 cooperate with GIGANTEA (GI) to promote CO gene activation [16,17], while the E3 ligases CONSTITUTIVE PHOTOMORPHOGENIC 1 (COP1) and HIGH EXPRESSION OF OSMOTICALLY RESPONSIVE GENE1 (HOS1) specifically target CO for breakdown during nighttime and dawn phases, respectively [8,9]. Additional factors like FLAVIN-BINDING, KELCH REPEAT, and F BOX 1 (FKF1) facilitate the removal of CYCLING DOF FACTOR 1 (CDF1) to maintain rhythmic CO production [18–20]. The regulation of CO protein stability and transcriptional activity involves additional components including PHYTOCHROME-ASSOCIATED LATE-FLOWERING (PHL) and EARLY ACTIVATION TARGET 1 (TOE1), which collectively fine-tune floral transition timing [18,21,22]. Earlier work revealed that ABI5-INTERACTING PROTEIN 2 (AFP2) promotes CO turnover through direct interaction, resulting in delayed flowering [23]. These observations establish that CO abundance and activity integrate diverse environmental signals at both transcriptional and post-translational levels. The NAC (NAM/ATAF/CUC) family represents one of the most extensive groups of transcriptional regulators in plants [24,25], with members governing fundamental developmental processes ranging from flower morphogenesis and cell division to cuticle formation and hair cell differentiation [25]. Emerging research underscores their pivotal roles in abiotic stress adaptation. Arabidopsis contains 117 NAC genes, including 14 membrane-associated members designated as NTL proteins [26,27], which exhibit specialized functions. NAC TRANSMEMBRANE MOTIF1 (NTM1) enhances pathogen defense [28], whereas NTL4 mediates drought-associated leaf aging [29]. ANAC089/NTL14 modulates ER stress-related cell death and flowering time via FLC regulation [30,31], while ANAC013/NTL1 participates in oxidative stress responses [32]. Particularly, NTL8 influences flowering through BFT interaction and regulates salt-stress germination [33]. Subsequent findings demonstrated its role in epidermal patterning through TRY and TCL1 targeting [34], along with contributions to cold adaptation and salinity tolerance during germination [35]. However, the detailed pathways through which NTL8 modulates floral induction require comprehensive exploration.

In this study, we examined how NTL8 influences floral timing, discovering its mRNA abundance follows daily rhythmic changes with maximal accumulation preceding sunset and gradual reduction during nocturnal and early daylight periods, closely resembling CO's transcriptional rhythm. Experimental data demonstrated NTL8 delays floral transition in extended photoperiods through FT repression, while protein interaction studies established its physical association with CO, indicating their cooperative regulation of FT levels to adjust flowering to day length. These results uncover a previously unknown role for NTL8 in floral timing control and provide mechanistic insights into how the NTL8-CO partnership operates within the light cycle-dependent flowering network.

2 Materials and Methods

2.1 Plant Material and Growth

The plant materials employed in this research, comprising the Arabidopsis thaliana T-DNA insertion lines *ntl8-1* (WiscDsloxHs159_07E) and *ntl8-2* (SM_3_16309), were generously supplied by Prof. Shucai Wang from Linyi University [34], while the *ft-10* line was obtained from Dr. Leiyin Zheng at the Chinese Academy of Sciences. Hybrid plants containing multiple mutations or transgenes were created through genetic crosses followed by isolation of pure-breeding offspring. For cultivation, sterilized seeds were placed on 0.5× MS plates containing 8 g/L agar and 10 g/L sucrose (adjusted to pH 5.7), with young plants maintained at 22°C

under either extended (16-h illumination at 100 μmol·m^{-2}·s^{-1}/8-h dark) or reduced (8-h light/16-h dark) daily light periods. Mature specimens were transplanted into a 3:1 soil-vermiculite mixture under controlled temperature conditions. The timing of floral transition was assessed by enumerating basal leaves when the primary stem elongated to 1–3 cm, with phenotypic analysis performed on 20–30 individuals per genetic variant.

2.2 Plasmid Construction and Transgenic Plants

The *35S::CO-Flag* fusion was created by PCR amplification of the complete *CO* coding region with PrimeSTAR DNA polymerase (Takara, Japan), followed by ligation to a Flag tag sequence. This amplicon was subsequently inserted into the *pRI101-AN* plasmid through In-Fusion HD cloning (Clontech, USA). The engineered vector was transferred into Arabidopsis Col-0 ecotype via Agrobacterium transformation, with transformants identified by growth on 0.5× MS plates supplemented with 50 μg/mL kanamycin [36]. Oligonucleotide sequences employed for molecular cloning appear in Supplementary Table S1.

2.3 Protein Immunoblots Analysis

Plant tissue proteins were isolated from young plants according to established protocols [37,38]. Cellular proteins were obtained with a lysis solution comprising 50 mM Tris-HCl (pH 7.5), 150 mM sodium chloride, 1 mM EDTA (pH 8.0), 0.1% Triton X-100, 10 mM sodium fluoride, and 5% glycerol, enhanced with phosphatase inhibitors (Roche) and 1 mM PMSF (Sigma). After centrifugation at 15,000× *g* for 10 min at 4°C, supernatants were collected for quantification with Bradford assay (Invitrogen). Protein samples (15 μg per lane) were resolved on 12% SDS-PAGE gels and electroblotted onto PVDF membranes, which were subsequently incubated with specific primary antibodies, including CO antibody (1:1000, Cat. 220746, Orizymes) generated against CO-His fusion protein, HA antibody (1:3000 dilution, Roche), FLAG antibody (1:3000, Sigma), GFP antibody (1:3000, Clontech), or actin antibody (1:1000, Sigma), followed by HRP-linked anti-mouse or anti-rat IgG (1:3000, Promega). Immunoreactive bands were visualized using an enhanced chemiluminescence detection system (Genescript).

2.4 Yeast Two-Hybrid Assays

To conduct yeast two-hybrid analysis, the gene fragment containing *NTL8* and *CO* were PCR-amplified and subsequently inserted into pGBKT7 (DNA-binding domain vector) and pGADT7 (activation domain vector) respectively through In-Fusion cloning technology (Clontech) [23,38]. Y187 and AH109 yeast cells were genetically modified with the activation domain and DNA-binding domain constructs correspondingly via polyethylene glycol transformation following standard procedures. Following selection on tryptophan-deficient (630413, Clontech) or leucine-deficient (630414, Clontech) agar plates, three separate colonies per plasmid combination were crossed and cultured on double dropout medium (630417, Clontech) for 72 h to verify mating efficiency. The resulting diploid strains were then plated on quadruple dropout selection plates (630428, Clontech) to assess potential molecular interactions through colony formation.

2.5 In Vitro Pull-down Assays

To examine protein interactions *in vitro*, complete or partial coding sequences of *NTL8* and *CO* were PCR-amplified and subsequently inserted into pET28a (Merck) and pGEX-4T-1 (Pharmacia) expression vectors, creating *pET28a-CO* and *pGST-NTL8* recombinant plasmids [23]. Oligonucleotides employed for amplification are provided in Supplementary Table S1. For bacterial protein production, these plasmids were introduced into *E. coli* Rosetta cells, with recombinant protein synthesis initiated by IPTG treatment. The

expressed GST-fused NTL8 was purified using glutathione-coupled resin (GE Healthcare), while GST protein served as negative control. In binding experiments, 2 μg of His-tagged CO was mixed with either GST or GST-NTL8 bound to beads in interaction solution (50 mM Tris-HCl, pH 8.0, 100 mM NaCl, 1 mM EDTA) at 4°C for 12 h. Following incubation, captured complexes were rigorously rinsed with wash buffer (50 mM Tris-HCl, pH 7.4, 100 mM NaCl, 0.6% Triton X-100). Resolved proteins from 8% SDS-PAGE were transferred to membranes and analyzed by western blotting with His-specific (Abmart) or GST-specific (Abmart) antibodies, then visualized using HRP-conjugated anti-mouse IgG (1:5000; Promega).2.6 Co-immunoprecipitation.

2.6 Co-Immunoprecipitation

To investigate protein interactions in planta, *NTL8-HA* and *CO-Flag* lines were crossed to create dual-expressing transgenic plants. For co-immunoprecipitation experiments with CO-FLAG as the target, 14-day-old *NTL8-HA/CO-Flag* seedlings were cryogenically pulverized [23]. Cellular proteins were isolated with extraction buffer containing 100 mM MOPS (pH 7.6), 150 mM sodium chloride, 0.1% NP-40, 1% Triton X-100, 20 mM iodoacetamide, 1 mM PMSF, protease inhibitors (2 μg/mL aprotinin, 5 μg/mL leupeptin, 1 μg/mL pepstatin) and phosphatase inhibitors (Roche). After centrifugation at 22,000× *g* (4°C, 10 min) and Miracloth filtration, 1 mL cleared lysate was mixed with HA-conjugated magnetic beads (Sigma) for 2 h at 4°C with rotation. Following four washes with 50 mM Tris (pH 8.0), 150 mM NaCl, 0.1% Triton X-100, captured complexes were heat-eluted (95°C, 10 min) in SDS sample buffer (100 mM Tris-HCl pH 6.8, 200 mM DTT, 2% SDS, 20% glycerol, 0.2% bromophenol blue). Immunodetection was performed using FLAG (1:3000, Sigma) or HA (1:3000, Roche) antibodies, with NTL8-HA/GFP-Flag plants serving as negative controls.

2.7 RT-qPCR Analysis

Total RNA was isolated from two-week-old seedlings with TRIzol (Invitrogen), followed by cDNA synthesis from 1.5 μg DNase-digested RNA in 20 μL reactions employing M-MuLV reverse transcriptase (Fermentas) and oligo(dT)18 primers [23,38]. Quantitative PCR analysis was conducted using diluted cDNA (2–10 ng/μL) with SYBR Green Master Mix on a LightCycler 480 system (Roche) according to standard protocols, with *PP2A* serving as the reference gene. Three technical replicates were performed for each assay, with primer sequences provided in Supplementary Table S1.

2.8 Protoplast Transient Expression Assay

To analyze transient gene expression in Arabidopsis protoplasts, a 2.7-kb *FT* promoter fragment was ligated into *pGreenII 0800-LUC* to create FTpro::LUC reporter plasmids, while *NTL8* and *CO* coding sequences were subcloned into pGreenII 62-SK downstream of the *35S* promoter (primer details in Supplementary Table S1). Leaf mesophyll protoplast isolation and transformation followed established protocols with slight adjustments. Luminescence measurements employed the dual-luciferase system (Promega), where firefly LUC activity was normalized to *35S*-driven Renilla luciferase (REN) from the same vector, with LUC/REN ratios determining relative expression levels.

2.9 Luciferase Complementation Imaging (LCI) Assay

To examine protein-protein interactions through luciferase complementation imaging, *NTL8* and *CO* coding sequences were inserted into pCAMBIA1300-nLUC and pCAMBIA1300-cLUC plasmids respectively, then introduced into *Agrobacterium GV3101*. Bacterial suspensions carrying these constructs were pressure-infiltrated into Nicotiana benthamiana foliage, with luminescence signals captured 48 h

post-infiltration using a Tanon 5200 cooled-CCD imaging platform (Shanghai), following established methodology [39].

2.10 Chromatin Immunoprecipitation Following by qPCR Analysis (CHIP-qPCR)

To analyze histone modifications, 14-day-old LD-grown seedlings were collected at ZT16 (light-off transition) and immediately vacuum-infiltrated for 15 min with fixation solution containing 10 mM Tris-HCl (pH 8.0), 0.4 M sucrose, 1 mM EDTA, 1 mM PMSF, 0.25% Triton X-100, and 1% formaldehyde. The reaction was stopped with 0.125 M glycine under vacuum for 10 min, followed by three washes with chilled water. Frozen tissues were pulverized in liquid nitrogen, and chromatin was isolated, sonicated to 300–500 bp fragments, then incubated with Protein A/G magnetic beads coupled with anti-acetyl-H3 antibody (Abcam #ab47915) recognizing multiple lysine residues (K9/14/18/23/27). After 5-h elution at 65°C, immunoprecipitated DNA was purified (NEB kit) and quantified by qPCR (LightCycler 480, SYBR Green), with enrichment values calculated by normalizing against input DNA and wild-type controls (primers in Supplementary Table S1).

3 Results

3.1 Circadian Expression of NTL8

To investigate the expression pattern of *NTL8* during both daytime and nighttime, two-week-old seedlings were subjected to long-day (LD) photoperiodic conditions (16-h light, 8-h darkness), and the transcriptional level of *NTL8* was measured at 4-h intervals. As shown in Fig. 1A, the expression of *NTL8* showed rhythmic oscillations, with a gradual increase during the daytime, reaching a peak at ZT16, coinciding with dusk, and then decreasing during the nighttime. Similarly, when seedlings were grown under short-day (SD) photoperiodic conditions (8-h light, 16-h darkness), rhythmic expression of *NTL8* was still observed, with a peak at ZT8, followed by sustained low expression level during the nighttime. Notably, the maximum transcriptional level of *NTL8* under SD conditions was lower than that observed under LD conditions during the daytime. These data suggest the circadian oscillation of *NTL8*, and indicate that light conditions induced the expression of *NTL8*, while darkness suppressed the expression. To further test this hypothesis, we shifted seedlings from constant dark (cD) conditions to light conditions (L), resulting in the induced expression of *NTL8* (Fig. 1B). Conversely, when shifting the seedlings from constant light conditions (cL) to dark conditions (D), *NTL8* expression was downregulated (Fig. 1B). These data confirm that the expression of *NTL8* is light-inducible and presents a circadian rhythm.

3.2 NTL8 Regulates Flowering Time

Most circadian-regulated genes are known to influence flowering time [1,6,7,12]. To investigate the potential role of *NTL8* in flowering time regulation, we obtained two T-DNA insertion lines, in which T-DNA insertions disrupted the second and third exons, respectively, thereby impairing its functional transcript (Supplementary Fig. S1A,B). These two mutant lines were named *ntl8-1* and *ntl8*-2, respectively. In parallel, we obtained several independent transgenic lines overexpressing an *NTL8-HA* fusion gene under the control of constitutive *35S* promoter (*35S: NTL8-HA*, abbreviated as *NTL8*-HA, Supplementary Fig. S1C). Under long day (LD) conditions (16-h light/8-h dark), the flowering time of *ntl8* mutant lines was slightly earlier compared to wild-type Col line, while the flowering time of *NTL8-HA* was significantly later than that in the wild-type Col line (Fig. 2A). In contrast, no significant differences in flowering time were observed among Col, *ntl8* mutants, and *NTL8-HA* transgenic lines under short day (SD) conditions (8-h light/16-h dark, Fig. 2A). These findings suggest that NTL8 delays the flowering time via the photoperiodic pathway.

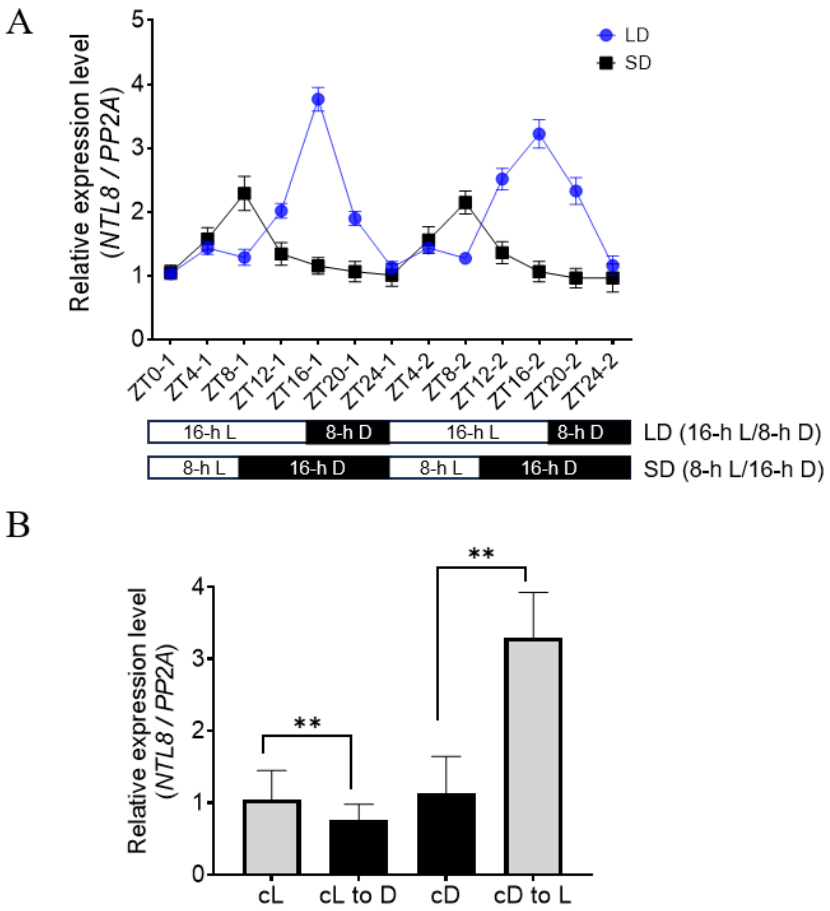

Figure 1: The circadian expression of *NTL8* by RT-qPCR analysis. (**A**) Two-week-old wild-type Col seedlings grown under long-day (LD) or short-day (SD) conditions were sampled for RT-qPCR analysis. *PP2A* is used as an internal control ($n = 3$, mean ± SD). (**B**) Light-responsive *NTL8* expression was examined in Col seedlings subjected to four light treatments: continuous light (cL, 24 h), continuous darkness (cD, 24 h), light-to-dark transition (12 h darkness after cL), and dark-to-light transition (12 h light after cD), followed by RT-qPCR analysis ($n = 3$, mean ± SD, $^{**}p < 0.01$ by Student's *t*-test).

FLOWERING LOCUS T (*FT*) acts as a mobile florigen that promotes flowering in *Arabidopsis thaliana* [1,2,14]. To determine whether NTL8 acted through the regulation of *FT* we compared the expression levels of *FT* in wild-type Col, *ntl8* mutants (*ntl8-1* and *ntl8-2*), and the *NTL8-HA* transgenic line (the line #1 was used hereafter) under long-day (LD) conditions. As shown in Fig. 2B, the transcriptional level of *FT* in both *ntl8-1* and *ntl8-2* mutants were higher than that in *NTL8-HA* line, compared to the wild-type Col line. These expression dynamics correlated with the observed flowering time phenotype of *ntl8* mutant and *NTL8-HA* lines, which supported the hypothesis that *NTL8* affected flowering time by regulating *FT* expression. To further validate this relationship, we crossed *ntl8-1* mutant and *NTL8-HA* line with the late-flowering *ft-10* mutant to obtain the *ntl8/ft* and *NTL8-HA/ft* lines. Under LD conditions, both lines exhibited a late-flowering phenotype, similar to *ft-10* mutant (Fig. 2C). Thus, these data confirm our previous hypothesis that *NTL8* requires *FT* signal to control flowering time under LD conditions.

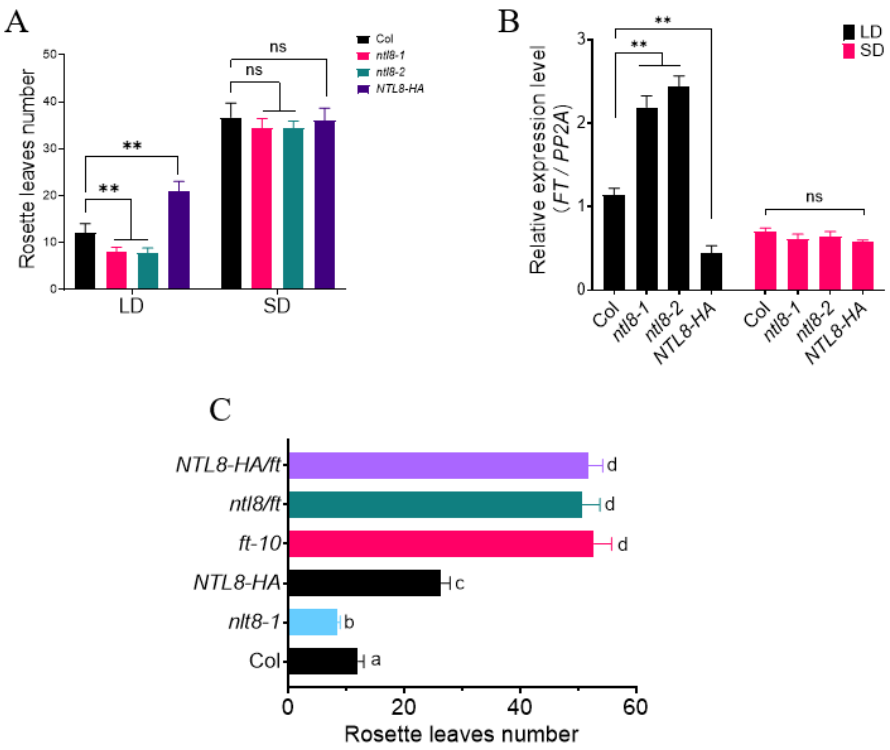

Figure 2: *NTL8* controls the flowering time through *FT* signal pathway. (**A**) Flowering time variation in *Col*, *ntl8* and *NTL8-HA* under LD/SD conditions. Plants were grown under LD (16 h light/8 h dark) or SD (8 h light/16 h dark) conditions, with flowering time determined by total rosette leaves number at bolting) (n = 3, mean ± SD; $^{**}p < 0.01$, t-test). (**B**) *FT* expression differences in Col, *ntl8* and *NTL8-HA* under LD/SD. Two-week-old seedlings grown under LD or SD were sampled at ZT16 (LD) or ZT8 (SD) for RT-qPCR analysis, *PP2A* was used as internal control; n = 3, mean ± SD; $^{**}p < 0.01$, t-test). (**C**) Flowering time comparison among Col, *ntl8* and *NTL8-HA* under LD. Flowering was assessed by total rosette leaves number at bolting (n = 3, mean ± SD). Different letters indicate significant differences ($p < 0.05$, ANOVA with Tukey's test).

3.3 NTL8 Interacts with CO

CO controls the expression of *FT* to accelerate flowering during photoperiod-dependent flowering pathway [1,6,7]. Given that NTL8 also modulates flowering time via the photoperiodic pathway, we sought to investigate the potential interaction between NTL8 and CO. To this end, we first checked their physical interaction. In yeast two-hybrid assays, yeast cells co-transformed with *NTL8* and *CO* constructs were able to grow on the selective medium lacking Trp/Leu/His/Ade (-LWHA), suggesting a direct interaction between the two proteins in yeast (Fig. 3A). This interaction was further supported by *in vitro* pull-down assays, in which *NTL8-GST* was co-immunoprecipitated with His-CO protein extracted from bacterial lysates, whereas GST alone did not interact with His-CO (Fig. 3B). To confirm this interaction *in planta*, we also checked the interaction between *NTL8* and *CO* in plant cells. As shown in Fig. 3C, we crossed the *NTL8-HA* transgenic line with *CO-Flag* line to obtain *NTL8-HA/CO-Flag* plants. As a negative control, we crossed the transgenic *GFP-Flag* line with *NTL8-HA* to obtain *GFP-Flag/NTL8-HA* plants. Total protein was extracted from the *NTL8-HA/CO-Flag* line and immunoprecipitated using anti-HA resin. A strong immunoblotting signal for *CO-Flag* was detected in the immunoprecipitated complex from the *NTL8-HA/CO-Flag* using an anti-Flag antibody, whereas GFP protein was not detected in the control immunoprecipitate from the *GFP-Flag/NTL8-HA* line. Thus, these results indicated that *NTL8* interacted with CO *in vitro* and *in*

vivo. To further confirm this interaction, we performed a luciferase complementation imaging (LCI) assay in *Nicotiana benthamiana* leaves. A strong bioluminescent signal was observed in leaves co-expressing *CO-nLuc*, and *cLuc-NTL8*, but not in those co-expressing the combination of *CO-nLuc* with *cLUC*, or *nLUC* with *CO-cLuc* (Fig. 3D). Collectively, these data provided strong evidence of the interaction of NTL8 and CO *in planta*.

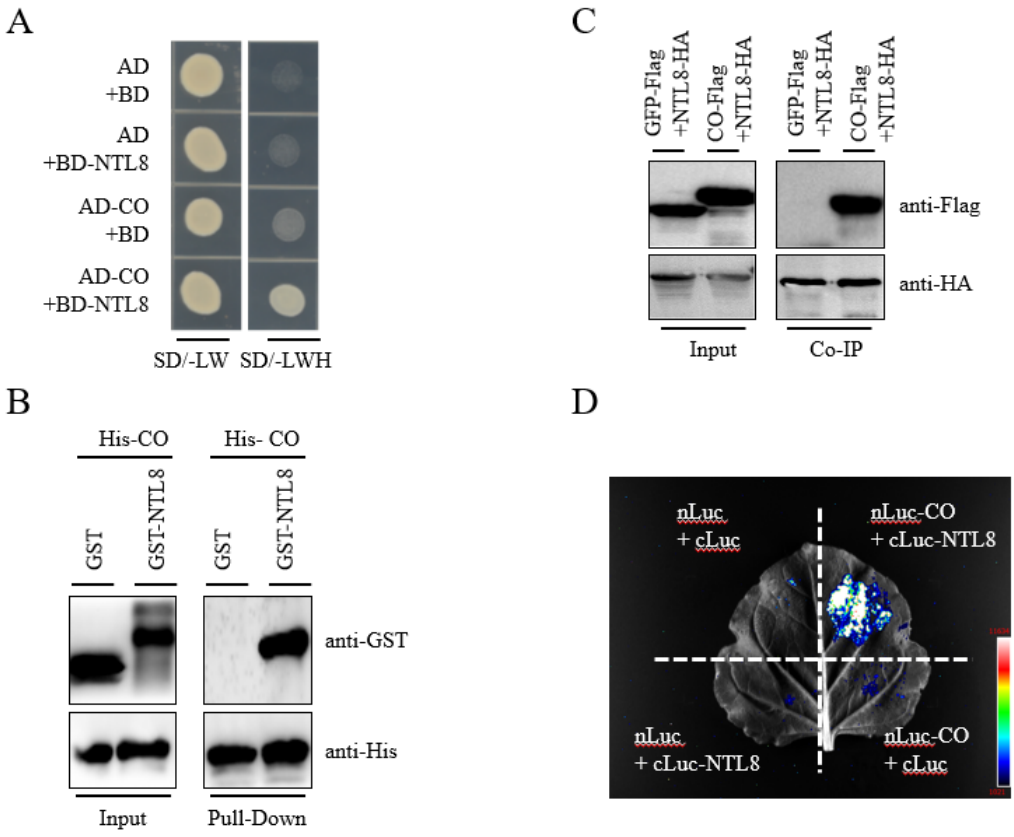

Figure 3: Interaction between *NTL8* and *CO in vitro* and *in planta*. (**A**) Y2H assay for NTL8-CO interaction. Yeast carrying AD/BD constructs were grown on -LW or -LWH medium. (**B**) *In vitro* pull-down of His-CO with GST-NTL8. GST served as control; bound proteins detected by anti-His/GST. (**C**) Co-IP of NTL8-CO in Arabidopsis. HA-resin precipitated proteins from CO-Flag/NTL8-HA seeds, detected by anti-Flag/HA. GFP-Flag/NTL8-HA as control. (**D**) LCI assay in N. benthamiana. CO-nLUC and NTL8-cLUC were co-expressed; luminescence imaged at 48 h post-infiltration (n = 3).

3.4 NTL8 Affects the Protein Stability of CO

Given that NTL8 interacts with CO and delays flowering time, we hypothesized that *NTL8* might influence CO protein stability under LD conditions, thereby modulating the flowering time. To test this possibility, we checked the circadian accumulation of CO protein in the wild-type Col line and *NTL8-HA* genetic background. Using a commercial anti-CO antibody, we monitored the circadian expression of CO protein levels throughout the diurnal cycle, observing a characteristic circadian expression pattern: CO protein accumulated during the daytime, peaking prior to nightfall, and was rapidly degraded during the nighttime (Fig. 4A,B). Compared to the pattern observed in Col plants, the protein abundance of CO in the *NTL8-HA* plants was lower at several key time points under LD conditions: ZT0 (dawn), ZT4 (dawn) and ZT20 (nighttime). Notably, at ZT4 or ZT20 points, the protein levels of CO in *NTL8-HA* plants were

markedly lower than those in Col. However, CO protein levels at ZT12 and ZT16 did not show obvious differences between Col and *NTL8-HA* lines. We further compared CO protein accumulation among Col, *ntl8-1* mutants, and *NTL8-HA* plants across different time points (Fig. 5A,B). Under LD conditions, CO protein levels in *NTL8-HA* plants at ZT0, ZT4 and ZT20 were significantly lower than those in *ntl8-1* mutants or Col. In addition, a statistically significant differences in CO accumulation between *ntl8-1* mutants and Col plants was detected at ZT16 and ZT20 (Fig. 5A,B). These results suggested that *NTL8* regulates the protein stability of CO, thereby modulating flowering time under LD conditions. This finding was consistent with the observed flowering time phenotype and *FT* expression patterns in *ntl8-1* mutants and *NTL8-HA* line under LD conditions. Furthermore, we assessed *CO* accumulation pattern among Col, *ntl8-1* mutant, and *NTL8-HA* lines under short-day (SD) conditions. No significant differences were detected at different time points, although CO protein abundance in *NTL8-HA* plants was slightly lower than that in Col or *ntl8-1* mutants at ZT12 (Supplementary Fig. S2). These data further support the conclusion that *NTL8* affects *CO*-mediated flowering predominantly under LD conditions, in line with the absence of flowering time differences among the lines under SD conditions (Fig. 2A).

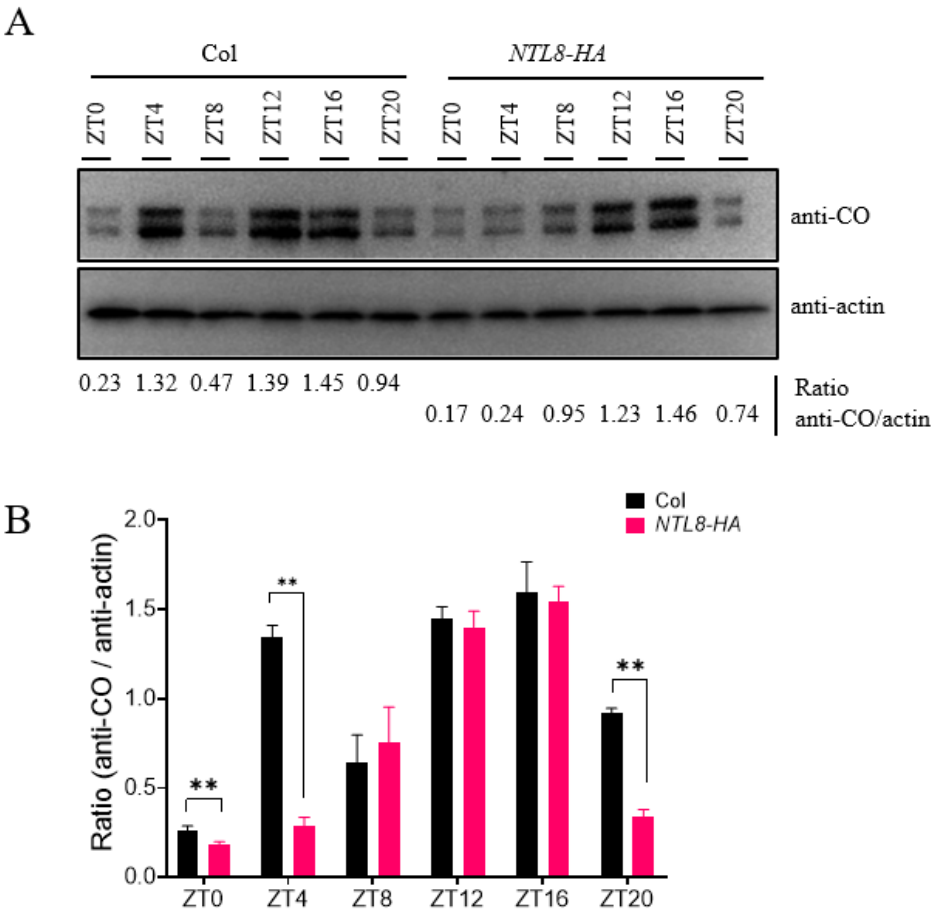

Figure 4: Diurnal oscillation of CO protein abundance in Col and *NTL8-HA* lines under LD conditions. (**A**) CO protein oscillation in Col and *NTL8-HA* under LD. Samples collected every 4 h (ZT0-24) for immunoblot (anti-CO/actin). The ratio of CO to Actin was evaluated by the immunoblot signal of anti-CO and anti-actin antibodies, and is listed at the bottom of the figure. (**B**) Quantified CO/Actin ratios in Col vs. *NTL8-HA*. Data from three replicates (mean ± SD; $^{**}p < 0.01$, *t*-test).

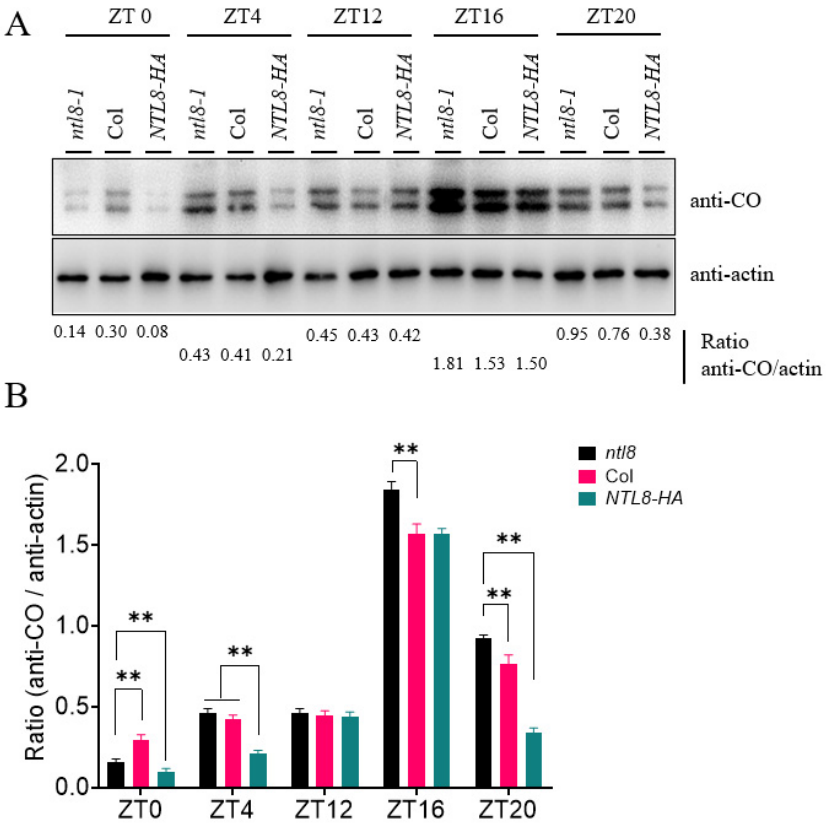

Figure 5: Differential oscillation of CO protein abundance among Col, *ntl8-1* and *NTL8-HA* lines under LD conditions. (**A**) CO protein levels in Col, *ntl8-1* and *NTL8-HA* at ZT4/12/16/22 (LD). The ratio of CO to Actin was evaluated by the immunoblot signal for anti-CO or anti-actin antibody, and is listed at the bottom of the figure. (**B**) Quantified CO/Actin ratios (Col vs. mutants). Data are presented as mean ± standard deviation (SD). Statistical differences were analyzed by Student's *t*-test analysis (**$p < 0.01$).

3.5 NTL8 Antagonizes the Effect of CO on Activating FT Expression

To better understand the genetic relationship between NTL8 and CO, we generated *CO-Flag/NTL8-HA* and *CO-Flag/ntl8* lines through reciprocal genetic crosses. As previously observed, the *NTL8-HA* line showed a late flowering phenotype characterized by an increased the rosette leaf number, whereas the *ntl8-1* mutant showed an early flowering phenotype with fewer rosette leaves (Fig. 2A). Consistent with previous results, the *CO-Flag* line also showed an early flowering phenotype with reduced rosette leaf number. In this study, we found that overexpression of *NTL8-HA* in the *CO-Flag/NTL8-HA* line partially delayed the early flowering phenotype of the *CO-Flag* line (Fig. 6A). Correspondingly, the *FT* expression level in *CO-Flag/NTL8-HA* plants at ZT16 was slightly lower than that in *CO-Flag* plants (Fig. 6B). These results suggest that *NTL8* antagonizes the early flowering phenotype of *CO-Flag* by suppressing *FT* expression. Furthermore, we observed that both of *CO-Flag/ntl8* and *ntl8-1* lines showed similar earlier flowering time (Fig. 6A), with elevated expression of *FT* at ZT16 under LD conditions, significantly higher than in *ntl8* plants. These findings indicated that inactivation of *NTL8* in *ntl8* mutant line further enhanced the effect of *CO-Flag* in promoting *FT* expression, supporting the notion of an antagonistic relationship between CO and NTL8 in regulating *FT* expression.

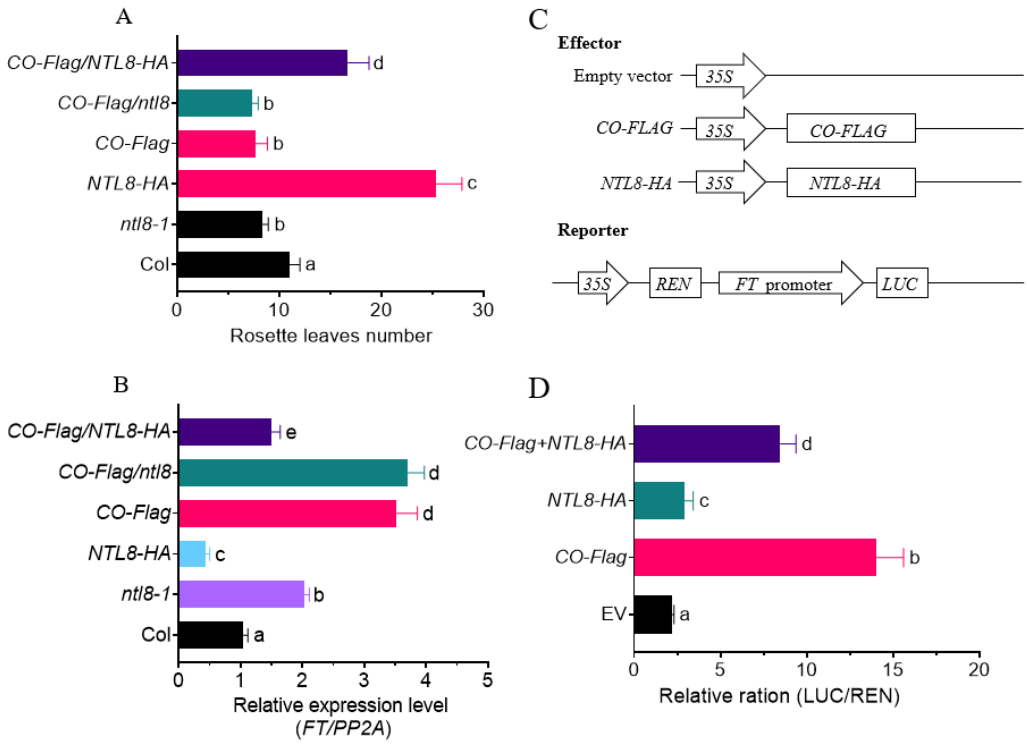

Figure 6: NTL8 and CO antagonistically regulate the expression of *FT* and flowering time. Bars labeled with different letters are significantly different at $p < 0.05$ (Tukey's test). (**A**) Different flowering time comparison among Col, *ntl8-1*, *NTL8-HA* and different crossed line under LD. ($n = 3$, mean ± SD). (**B**) *FT* expression levels among Col, *ntl8-1*, *NTL8-HA* and different crossed line under LD at ZT16 by RT-qPCR analysis. ($n = 3$, mean ± SD). PP2A was used as the internal control. (**C**) Schematic diagram of the effector and reporter constructs used in the transient transactivation assay. The reporter contains *FT*-promoter-driven Luciferase genes. (**D**) NTL8 modulates CO-activated *FT* expression by transient expression assay. The firefly luciferase and Renilla luciferase (LUC: REN) ratio represents *FTpro:LUC* activity relative to the internal control (*35Spro: REN*). ($n = 3$, mean ± SD).

Since CO directly binds to the promoter of *FT* to activate its expression, whereas NTL8 suppresses the expression of *FT*, this suggests an antagonistic relationship between CO and NTL8 in regulating *FT* expression. To test this hypothesis, we performed transient protoplast transformation assays to evaluate the effect of NTL8 on CO-mediated activation of *FT* expression in Arabidopsis leaf protoplasts. As shown in Fig. 6C,D, CO efficiently activated *FT* expression; however, this activation was attenuated when *NTL8-HA* was co-expressed with *CO-Flag* effector. As a control, expression of *NTL8-HA* alone with the *FTpro::LUC* reporter also partially suppressed LUC expression (Fig. 6D). Collectively, these results confirmed that NTL8 antagonized CO to suppress *FT* expression, thereby delaying flowering time.

Previous studies have demonstrated that CO upregulates histone acetylation at the *FT* locus to epigenetically activate *FT* expression [1–7]. Given that NTL8 counteracts CO to suppress *FT* expression, we speculated that NTL8 may attenuate CO-mediated histone acetylation at the *FT* locus. To test this possibility, we performed ChIP-qPCR analysis to measure three different regions of the *FT* locus, including the P1 region near the transcription start site (TSS) (*FT-P*, −297 bp−128 bp upstream of the start codon), the P2 region within the first exon close to the start codon (*FT-E*, +17 bp to +221 bp downstream of start codon), and the P3 region within the first intron of *FT* genome (*FT-I*, +568 bp to +785 bp downstream of the start codon) (Fig. 7). These regions were previously reported to show increased histone acetylation

upon *CO* overexpression. Consistent with these findings, we observed a relatively higher level of histone acetylation at the *FT* locus in the *CO-Flag* line compared with Col wild type at ZT16 under LD conditions. In contrast, histone acetylation levels were lower in the *NTL8-HA* line and higher in the *ntl8-1* mutant line, which was consistent with the *FT* expression pattern and their different flowering time phenotypes. Furthermore, compared with *CO-Flag* line, overexpressing *NTL8* in *CO-Flag/NTL8-HA* reduced histone acetylation levels. On the contrary, silencing *NTL8* in the *CO-Flag/ntl8* line increased histone acetylation levels. These findings suggest that *NTL8* suppresses the expression of *FT* by modulating *CO*-mediated H3 acetylation levels at *FT* locus.

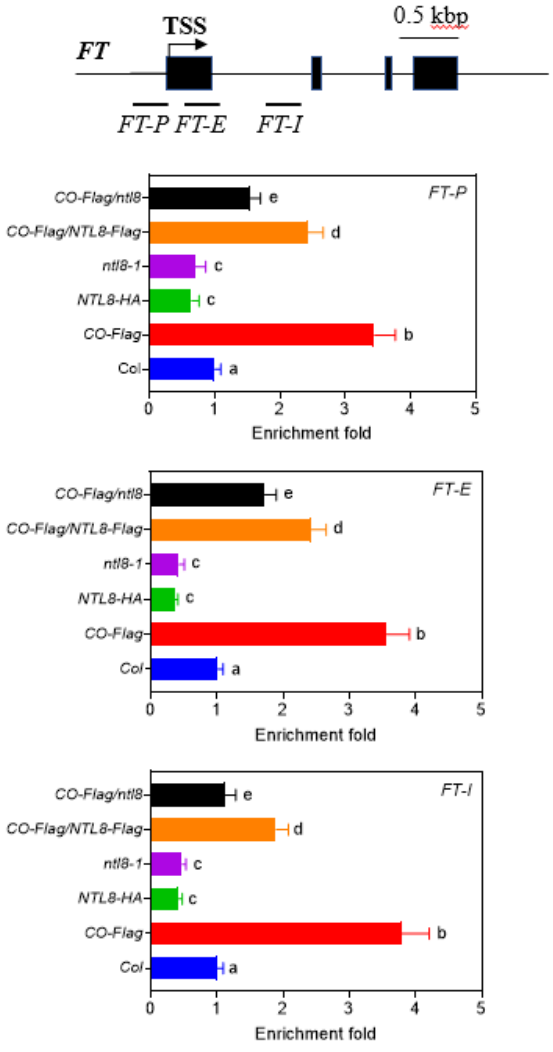

Figure 7: NTL8 represses CO-mediated upregulation of histone H3 acetylation level at the *FT* locus by ChIP-PCR analysis at the indicated regions (*FT-P*, *FT-E*, and *FT-L* fragments within the *FT* locus). The Col, *CO-Flag*, *NTL8-HA*, *ntl8-1*, *CO-Flag/NTL8-HA* and *CO-Flag/ntl8* lines were used. The seedlings were grown under LD conditions for 2 weeks and leaf samples were collected at ZT16 for ChIP-PCR analysis. An antibody against acetylated histone H3 was used for immunoprecipitation. *ACTIN2* was used as an internal control, and relative histone H3 acetylation levels at the *FT* locus were normalized to those of *ACTIN2*. The detailed positions of *FT-P*, *FT-E*, and *FT-L* are indicated by bars below the *FT* gene. Exons are shown as solid boxes, and introns as solid lines. Data are presented as mean ± standard deviation (SD) of three independent experiments. Bars with different letters indicate values that are significantly different at $p < 0.05$ (Tukey's test).

4 Discussion

4.1 NTL8 Acts As the Novel Modulator to Control Photoperiodic Flowering Time

Previous studies have reported that saline stress induced the expression of *NTL8* [33,36]. In the present study, we additionally demonstrated that *NTL8* was light-responsive and presented a circadian rhythm, with elevated transcript levels during the daytime and a marked reduction during the nighttime, similar to CO, the core regulator of the photoperiodic flowering pathway (Figs. 1 and 2). Consistent with prior findings, our data confirmed that NTL8 negatively controlled flowering time under long-day (LD) conditions, as overexpressing *NTL8* delayed flowering time, whereas loss-of-function mutant of *ntl8* showed earlier flowering than the wild type (Fig. 2). *FT* encodes a mobile florigen that promotes flowering time, and CO binds to the promoter of *FT* to activate its expression, thereby promoting flowering [1,14]. In line with this, we observed that *FT* transcript levels in *ntl8* were higher than that in *NTL8-HA* line (Fig. 2D). Genetic analysis further supported the conclusion that *NTL8* acted upstream of *FT* to regulate flowering time. Specifically, both of *ntl8/ft* double mutant and *NTL8-HA/ft* line showed later flowering time similar to that of the *ft-10* mutant (Fig. 2E), indicating that *NTL8* mediated photoperiodic flowering through targeting *FT*. Consistent with our findings, previous studies have shown that long-term cold treatment, or vernalization, efficiently suppresses the flowering time of the *NTL8-HA* line, similar to the wild-type Col line. Furthermore, a dominant mutation of *NTL8* was found to constitutively activate the expression of *VIN3*, leading to the silencing of *FLC* during vernalization, suggesting a complex role for *NTL8* in controlling flowering time in response to cold conditions [36]. Given that both NTL8 and NTL14 contain transmembrane domain (TMD) and cooperatively modulate seed dormancy [40], and that NTL14 has also been reported to control flowering time by modulating *FLC*, the negative component for flowering time [31], it is plausible that NTL8 may similarly influence the expression of *FLC* to control flowering time. Moreover, ANAC060, which contained TMD and is clustered into the same phylogenetic clade as NTL8, ANAC060 suppresses the expression of *ABI5*, which is the essential signal transmitter of ABA signaling [39–41]. Since ABI5 also plays a role in modulating flowering time, it would be interesting to investigate whether *NTL8* controls flowering time through an *ABI5*-dependent pathway [39,41]. Similar to cold treatment, GA treatment reversed the later-flowering phenotype of *NTL8-HA* line. Interestingly, GA treatment can reduce the expression of *NTL8*, and the seed germination of *ntl8* showed increased tolerance to GA biosynthesis inhibitors [33,36], suggesting distinct functions of NTL8 in seed germination and flowering time regulation. In contrast, saline treatment induces the expression of *NTL8*, and overexpressing *NTL8* delayed the flowering time, consistent with the late-flowering phenotype of *NTL8-HA* transgenic plant under salt stress. As previous studies reported that saline stress reduces *FT* expression, we also observed lower *FT* expression level in the *NTL8-HA* line (Fig. 2), supporting the hypothesis that salt stress delays flowering time by activating *NTL8* and subsequently reducing *FT* signaling. Furthermore, since salt stress has been shown to induce the expression of *BFT*, which competes with *FT* for *FD* bindings and suppresses the activity of *FT* [36], it will be important to further investigate whether saline-induced flowering delay involves *NTL8*-mediated regulation of *BFT*.

4.2 NTL8 Interacts with CO to Influence Its Transactivation to FT Expression

CO acts as a central hub in the photoperiodic flowering regulatory network [1,6]. Its transcription presented a circadian rhythm, and its protein abundance also showed rhythmic oscillation, accumulating during the daytime to efficiently activate *FT* expression and subsequently being degraded by the E3 ubiquitin ligase COP1 during the night [8]. Our previous research showed that the ABA associated protein AFP2

epigenetically repressed the transcriptional level of *CO* and promoted its proteasomal degradation, thereby delaying flowering time in Arabidopsis [39]. In the present study, multiple lines of evidence, including yeast two hybrid, *in vitro* pull-down assays, and *in vivo* CO-IP, confirmed the physical interaction between CO and NTL8 (Fig. 3). Genetic analysis further revealed that the *ntl8* mutant exhibited an early-flowering phenotype, while the *NTL8-HA* line showed a delayed-flowering phenotype under LD conditions, but not under SD conditions (Fig. 2), suggesting a photoperiodic-dependent regulatory role. Moreover, overexpressing *NTL8* delayed the early-flowering phenotype of *CO-Flag* (Fig. 6), further supporting an antagonistic interaction between NTL8 and CO in controlling photoperiodic flowering time. Consistent with this, transient protoplast transformation assays showed that overexpressing *NTL8* attenuated the transcriptional action of CO on *FT* expression (Fig. 6), providing mechanistic insights into how *NTL8* antagonizes the acceleration effect of CO on *FT* expression. In addition, our results showed the circadian oscillation of *NTL8* transcript, with high transcript levels during the daytime and declining during the nighttime (Fig. 1). This diurnal expression pattern of *NTL8* suggests that it may fine-tune CO activity by repressing *FT* expression during the day, thereby contributing to the precise temporal regulation of flowering time.

The NTL8 homolog ANAC089 has been reported to bind to the promoter of *FLC* to suppress its expression, thereby promoting earlier flowering [31]. Similarly, another homolog, ANAC060 binds to the promoter of *ABI5* to suppress its expression and attenuate ABA signaling [40]. However, in the case of NTL8, we found no direct evidence of binding of NTL8 to *FT* promoter, although *NTL8* clearly influenced *FT* expression. One possible explanation for this discrepancy lies in the complex and highly variable presence of cis-elements within the promoter of *FT*. Previous studies have reported that key enhancer elements of *FT* can reside more than 10 kb upstream from the start codon [42], suggesting that our inability to detect the direct binding of NTL8 may be due to not targeting the correct cis-regulatory region within the *FT* promoter. Additionally, previous studies have demonstrated that histone deacetylase (HDAC) complexes, such as those containing SAP30 function-related proteins 1/2 (AFR1/2) epigenetically decreases *FT* transcription at the end of day by reducing acetylation level at *FT* locus, Furthermore, CO was shown to interact with MRG1/2, which then recruits the histone deacetylase HADC to reduce the histone acetylation level at the *FT* locus, thereby reducing its expression. These findings raise the possibility that NTL8 suppresses the expression of *FT* through a similar epigenetic mechanism. In support of this hypothesis, we observed that overexpression of *NTL8* in *CO-Flag* genetic background reduced histone acetylation level at the *FT* locus, whereas silencing *NTL8* in the *CO-Flag* genetic background line led to an increase in acetylation levels at the *FT* locus (Fig. 7). Collectively, these results suggest that NTL8 may recruit HDAC complexes to the *FT* locus to epigenetically reduce its expression at dusk, providing a mechanistic explanation for the antagonistic relationship between NTL8 and CO in regulating *FT* expression and flowering time.

In addition to the circadian rhythm observed at the transcript level, the protein abundance of CO also presented a circadian pattern, characterized by accumulation during the daytime, and degradation during the nighttime. Several E3 ubiquitin ligases, such as HOS1 and COP1, have been reported to mediate CO degradation [8,11]. Our previous study showed that AFP2 interacts with CO and promotes its degradation during the night [23]. In the present study, we observed a relatively lower protein abundance of CO in the *NTL8-HA* line, particularly at ZT20 during the nighttime, where CO levels were markedly lower than those in wild-type Col plants. These findings suggest that overexpression of *NTL8* induced the protein degradation of CO during the night. It is possible that NTL8 synergistically enhanced the activity of E3 ligases, such as COP1, thereby promoting the degradation of CO during the nighttime. Further investigation will be necessary to elucidate whether, and through which mechanisms, NTL8 influences the protein abundance and stability of CO via specific E3 ligases such as COP1. Notably, the reduced protein abundance of CO observed

at ZT4 (dawn) in the *NTL8-HA* transgenic line may explain the reduced *FT* expression observed in these plants. This finding suggested that NTL8 may also suppress CO accumulation during the daytime. Previous studies have reported that the E3 ligase HOS1 also affects CO accumulation during dawn. Therefore, it is plausible that NTL8 influences CO accumulation in the morning through modulation of HOS1 activity. Nevertheless, further investigation will be required to clarify these potential regulatory mechanisms.

In summary, this study expanded our understanding of the role of NTL8 in the regulation of flowering time. Our results showed that NTL8 interacted with CO to suppress *FT* expression, thereby delaying flowering under long-day conditions. A combination of physiological, biochemical, and genetic analyses further supported that NTL8 antagonized CO function to suppress *FT* transcription. In addition, we found that NTL8 influenced the protein stability of CO during the nighttime, acting at a post-transcriptional level. Collectively, our findings contribute to a deeper understanding of the mechanisms underlying the CO-mediated photoperiodic flowering pathway, and suggest that the NTL8-CO module represents a novel regulatory mechanism that requires further attention, especially for its potential applications in the genetic modification of flowering time in horticultural research.

5 Conclusion

In this study, we performed genetic analysis to confirm that NTL8 negatively regulates flowering time in Arabidopsis, as overexpressing NTL8 delays flowering time but silencing NTL8 shows early flowering time. Further analysis shows NTL8 itself presents circadian expression, and NTL8 also interacts with CO, thereby destabilize CO stability to repress FT expression, resulting into late flowering. Thus, we propose a uncovered mechanism of NTL8 in coordinating flowering time through antagonizing CO to reduce FT expression.

Acknowledgement: We are grateful to Professor Shucai Wang at Linyi University (Shandong, China) and Dr. Leying Zheng in Institute of Botany (Chinese Academy of Sciences, China) for sharing the seeds.

Funding Statement: This work was supported by the National Natural Science Foundation of China (31970289).

Author Contributions: Yue Jin: investigation, methodology, resources, writing–original draft. Xiaoying Tang: investigation, methodology, conceptualization. Bingke Wei: methodology, validation. Lulu Zhi: investigation, methodology. Yan Mao: investigation, methodology. García-Caparrós Pedro: writing—original draft, writing—review & editing. Xiangyang Hu: conceptualization, methodology, resources, writing—original draft, writing—review & editing, supervision, funding acquisition, project administration. All authors reviewed and approved the final version of the manuscript.

Availability of Data and Materials: The authors confirm that the data supporting the findings of this study are available within the article.

Ethics Approval: Not applicable.

Conflicts of Interest: The authors declare no conflicts of interest.

Supplementary Materials: The supplementary material is available online at https://www.techscience.com/doi/10.32604/phyton.2026.067796/s1. Supplementary Table S1: List of primers used in this study. Supplementary Figure S1: Identification of *ntl8* mutant or *NTL8-HA* lines. (**A**,**B**) Verification of the *ntl8* mutant and its overexpressed lines. The genomic structure of *NTL8* gene and its T-DNA insertion (**A**). The location of T-DNA in the *ABI4* locus was detected by specific primers pairs (B);The expression of *NTL8-HA* in the transgenic line overexpressing *NTL8-HA* was detected by western blotting analysis using anti-HA antibody (**C**). Supplementary Figure S2: The dynamic change of *CO* abundance of Col, *ntl8-1* and *NTL8-HA* line under SD condition (8-h D/16-h L). (**A**) The leave samples

from wild-type Col, *ntl8* mutant and the transgenic *NTL8-HA* backgrounds were collected at ZT4, ZT12, ZT16 and ZT22 under SD conditions. The total proteins were extracted for CO protein abundance analysis and anti-actin was used as the internal control (upper panel). The ratio of CO to Actin was evaluated by the immunoblot signal for anti-CO and anti-actin, and is listed at the bottom of the figure. (**B**) The ratio of CO to Actin in the extracted protein wild-type Col, *ntl8* mutant and the transgenic *NTL8-HA* lines were evaluated by the immunoblot signal for anti-CO and anti-actin based on three individual western blotting experiments, and the quantification degree were presented. Three biological replications were performed. Data are presented as mean ± standard deviation (SD). Statistical differences were analyzed by *t*-test analysis, ns indicates that the result is not statistically significant.

References

1. Freytes SN, Canelo M, Cerdán PD. Regulation of flowering time: When and where? Curr Opin Plant Biol. 2021;63:102049. [CrossRef].
2. Johansson M, Staiger D. Time to flower: Interplay between photoperiod and the circadian clock. J Exp Bot. 2015;66(3):719–30. [CrossRef].
3. Jackson SD. Plant responses to photoperiod. New Phytol. 2009;181(3):517–31. [CrossRef].
4. Imaizumi T. *Arabidopsis* circadian clock and photoperiodism: Time to think about location. Curr Opin Plant Biol. 2010;13(1):83–9. [CrossRef].
5. Susila H, Nasim Z, Ahn JH. Ambient temperature-responsive mechanisms coordinate regulation of flowering time. Int J Mol Sci. 2018;19(10):3196. [CrossRef].
6. Shim JS, Kubota A, Imaizumi T. Circadian clock and photoperiodic flowering in *Arabidopsis*: CONSTANS is a hub for signal integration. Plant Physiol. 2017;173(1):5–15. [CrossRef].
7. Putterill J, Robson F, Lee K, Simon R, Coupland G. The CONSTANS gene of *Arabidopsis* promotes flowering and encodes a protein showing similarities to zinc finger transcription factors. Cell. 1995;80(6):847–57. [CrossRef].
8. Liu LJ, Zhang YC, Li QH, Sang Y, Mao J, Lian HL, et al. COP1-mediated ubiquitination of CONSTANS is implicated in cryptochrome regulation of flowering in *Arabidopsis*. Plant Cell. 2008;20(2):292–306. [CrossRef].
9. Lazaro A, Valverde F, Piñeiro M, Jarillo JA. The *Arabidopsis* E3 ubiquitin ligase HOS1 negatively regulates CONSTANS abundance in the photoperiodic control of flowering. Plant Cell. 2012;24(3):982–99. [CrossRef].
10. Cheng Z, Zhang X, Huang P, Huang G, Zhu J, Chen F, et al. Nup96 and HOS1 are mutually stabilized and gate CONSTANS protein level, conferring long-day photoperiodic flowering regulation in *Arabidopsis*. Plant Cell. 2020;32(2):374–91. [CrossRef].
11. Jung JH, Seo PJ, Park CM. The E3 ubiquitin ligase HOS1 regulates *Arabidopsis* flowering by mediating CONSTANS degradation under cold stress. J Biol Chem. 2012;287(52):43277–87. [CrossRef].
12. Takagi H, Hempton AK, Imaizumi T. Photoperiodic flowering in *Arabidopsis*: Multilayered regulatory mechanisms of CONSTANS and the florigen FLOWERING LOCUS T. Plant Commun. 2023;4(3):100552. [CrossRef].
13. Zhang B, Feng M, Zhang J, Song Z. Involvement of CONSTANS-like proteins in plant flowering and abiotic stress response. Int J Mol Sci. 2023;24(23):16585. [CrossRef].
14. Wigge PA. FT, a mobile developmental signal in plants. Curr Biol. 2011;21(9):R374–8. [CrossRef].
15. Miskolczi P, Singh RK, Tylewicz S, Azeez A, Maurya JP, Tarkowská D, et al. Long-range mobile signals mediate seasonal control of shoot growth. Proc Natl Acad Sci U S A. 2019;116(22):10852–7. [CrossRef].
16. Ito S, Song YH, Josephson-Day AR, Miller RJ, Breton G, Olmstead RG, et al. FLOWERING BHLH transcriptional activators control expression of the photoperiodic flowering regulator CONSTANS in *Arabidopsis*. Proc Natl Acad Sci U S A. 2012;109(9):3582–7. [CrossRef].
17. Kubota A, Ito S, Shim JS, Johnson RS, Song YH, Breton G, et al. TCP4-dependent induction of CONSTANS transcription requires *GIGANTEA* in photoperiodic flowering in *Arabidopsis*. PLoS Genet. 2017;13(6):e1006856. [CrossRef].
18. Song YH, Smith RW, To BJ, Millar AJ, Imaizumi T. FKF1 conveys timing information for CONSTANS stabilization in photoperiodic flowering. Science. 2012;336(6084):1045–9. [CrossRef].
19. Imaizumi T, Tran HG, Swartz TE, Briggs WR, Kay SA. FKF1 is essential for photoperiodic-specific light signalling in *Arabidopsis*. Nature. 2003;426(6964):302–6. [CrossRef].
20. Imaizumi T, Schultz TF, Harmon FG, Ho LA, Kay SA. FKF1 F-box protein mediates cyclic degradation of a repressor of CONSTANS in *Arabidopsis*. Science. 2005;309(5732):293–7. [CrossRef].

21. Endo M, Kudo D, Koto T, Shimizu H, Araki T. Light-dependent destabilization of PHL in *Arabidopsis*. Plant Signal Behav. 2014;9(3):e28118. [CrossRef].
22. Zhang B, Wang L, Zeng L, Zhang C, Ma H. *Arabidopsis* TOE proteins convey a photoperiodic signal to antagonize CONSTANS and regulate flowering time. Genes Dev. 2015;29(9):975–87. [CrossRef].
23. Chang G, Wang C, Kong X, Chen Q, Yang Y, Hu X. AFP2 as the novel regulator breaks high-temperature-induced seeds secondary dormancy through ABI5 and SOM in *Arabidopsis thaliana*. Biochem Biophys Res Commun. 2018;501(1):232–8. [CrossRef].
24. Mathew IE, Agarwal P. May the fittest protein evolve: Favoring the plant-specific origin and expansion of NAC transcription factors. Bioessays. 2018;40(8):e1800018. [CrossRef].
25. Chakraborty R, Roy S. Evaluation of the diversity and phylogenetic implications of NAC transcription factor members of four reference species from the different embryophytic plant groups. Physiol Mol Biol Plants. 2019;25(2):347–59. [CrossRef].
26. Kim SY, Kim SG, Kim YS, Seo PJ, Bae M, Yoon HK, et al. Exploring membrane-associated NAC transcription factors in *Arabidopsis*: Implications for membrane biology in genome regulation. Nucleic Acids Res. 2007;35(1):203–13. [CrossRef].
27. Kim SG, Lee S, Seo PJ, Kim SK, Kim JK, Park CM. Genome-scale screening and molecular characterization of membrane-bound transcription factors in *Arabidopsis* and rice. Genomics. 2010;95(1):56–65. [CrossRef].
28. Breeze E, Vale V, McLellan H, Pecrix Y, Godiard L, Grant M, et al. A tell tail sign: A conserved C-terminal tail-anchor domain targets a subset of pathogen effectors to the plant endoplasmic reticulum. J Exp Bot. 2023;74(10):3188–202. [CrossRef].
29. Lee S, Seo PJ, Lee HJ, Park CM. A NAC transcription factor NTL4 promotes reactive oxygen species production during drought-induced leaf senescence in *Arabidopsis*. Plant J. 2012;70(5):831–44. [CrossRef].
30. Albertos P, Tatematsu K, Mateos I, Sánchez-Vicente I, Fernández-Arbaizar A, Nakabayashi K, et al. Redox feedback regulation of ANAC089 signaling alters seed germination and stress response. Cell Rep. 2021;35(11):109263. [CrossRef].
31. Li J, Zhang J, Wang X, Chen J. A membrane-tethered transcription factor ANAC089 negatively regulates floral initiation in *Arabidopsis thaliana*. Sci China Life Sci. 2010;53(11):1299–306. [CrossRef].
32. De Clercq I, Vermeirssen V, Van Aken O, Vandepoele K, Murcha MW, Law SR, et al. The membrane-bound NAC transcription factor ANAC013 functions in mitochondrial retrograde regulation of the oxidative stress response in *Arabidopsis*. Plant Cell. 2013;25(9):3472–90. [CrossRef].
33. Kim SG, Lee AK, Yoon HK, Park CM. A membrane-bound NAC transcription factor NTL8 regulates gibberellic acid-mediated salt signaling in *Arabidopsis seed* germination. Plant J. 2008;55(1):77–88. [CrossRef].
34. Tian H, Wang X, Guo H, Cheng Y, Hou C, Chen JG, et al. *NTL8* regulates trichome formation in *Arabidopsis* by directly activating R3 MYB genes TRY and TCL1. Plant Physiol. 2017;174(4):2363–75. [CrossRef].
35. Zhao Y, Antoniou-Kourounioti RL, Calder G, Dean C, Howard M. Temperature-dependent growth contributes to long-term cold sensing. Nature. 2020;583(7818):825–9. [CrossRef].
36. Clough SJ, Bent AF. Floral dip: A simplified method for Agrobacterium-mediated transformation of *Arabidopsis thaliana*. Plant J. 1998;16(6):735–43. [CrossRef].
37. Ying S, Jing S, Cheng L, Sun H, Tian Y, Zhi L, et al. Allantoin alleviates seed germination thermoinhibition in *Arabidopsis*. Phyton. 2022;91(9):1893–904. [CrossRef].
38. Lu S, Hu Y, Chen Y, Yang Y, Jin Y, Li P, et al. Putrescine enhances seed germination tolerance to heat stress in *Arabidopsis thaliana*. Phyton. 2022;91(9):1879–91. [CrossRef].
39. Chang G, Yang W, Zhang Q, Huang J, Yang Y, Hu X. ABI5-BINDING PROTEIN2 coordinates CONSTANS to delay flowering by recruiting the transcriptional corepressor TPR2. Plant Physiol. 2019;179(2):477–90. [CrossRef].
40. Song S, Willems LAJ, Jiao A, Zhao T, Eric Schranz M, Bentsink L. The membrane associated NAC transcription factors ANAC060 and ANAC040 are functionally redundant in the inhibition of seed dormancy in *Arabidopsis thaliana*. J Exp Bot. 2022;73(16):5514–28. [CrossRef].
41. Wang Y, Li L, Ye T, Lu Y, Chen X, Wu Y. The inhibitory effect of ABA on floral transition is mediated by ABI5 in *Arabidopsis*. J Exp Bot. 2013;64(2):675–84. [CrossRef].
42. Cao S, Kumimoto RW, Gnesutta N, Calogero AM, Mantovani R, Holt BF 3rd. A distal ccaat/nuclear factor y complex promotes chromatin looping at the flowering locus t promoter and regulates the timing of flowering in *Arabidopsis*. Plant Cell. 2014;26(3):1009–17. [CrossRef].